Electronic Supplementary Information

Organic additive assisting with high ionic conduction and dendrite resistance of polymer electrolytes

Shundong Guan,[a] Kaihua Wen,[a] Ying Liang,[a] Chuanjiao Xue,[a] Sijie Liu,[a] Jinyao Yu,[a] Zheng Zhang,[a] Xinbin Wu,[a] Haocheng Yuan,[a] Zhiyuan Lin,[b] Haijun Yu,[b] Liangliang Li*[ac] and Ce-Wen Nan*[a]

a. State Key Laboratory of New Ceramics and Fine Processing, School of Materials Science and Engineering, Tsinghua University, Beijing 100084, China

b. Institute of Advanced Battery Materials and Devices, Faculty of Materials and Manufacturing, Beijing University of Technology, Beijing 100124, China

c. Key Laboratory of Advanced Materials (MOE), School of Materials Science and Engineering, Tsinghua University, Beijing 100084, China

* Corresponding author e-mail: liliangliang@mail.tsinghua.edu.cn (L. Li)
cwnan@mail.tsinghua.edu.cn (C.-W. Nan)

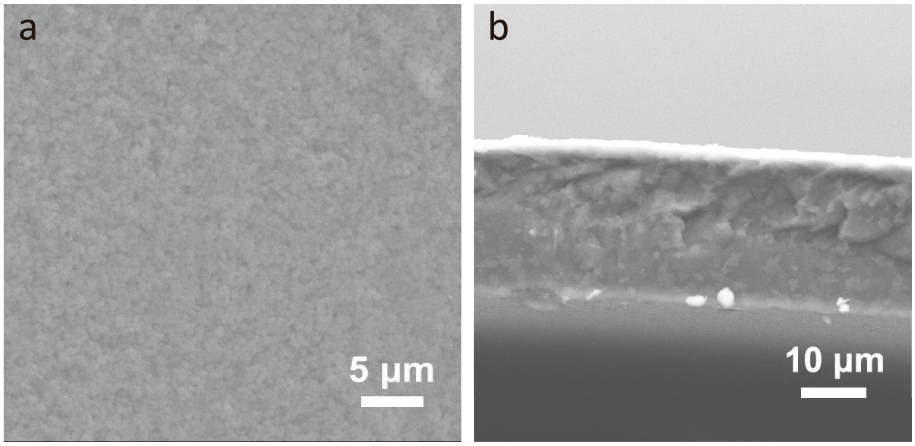

Fig. S1 (a) Top- and (b) side-view SEM images of the P-PE.

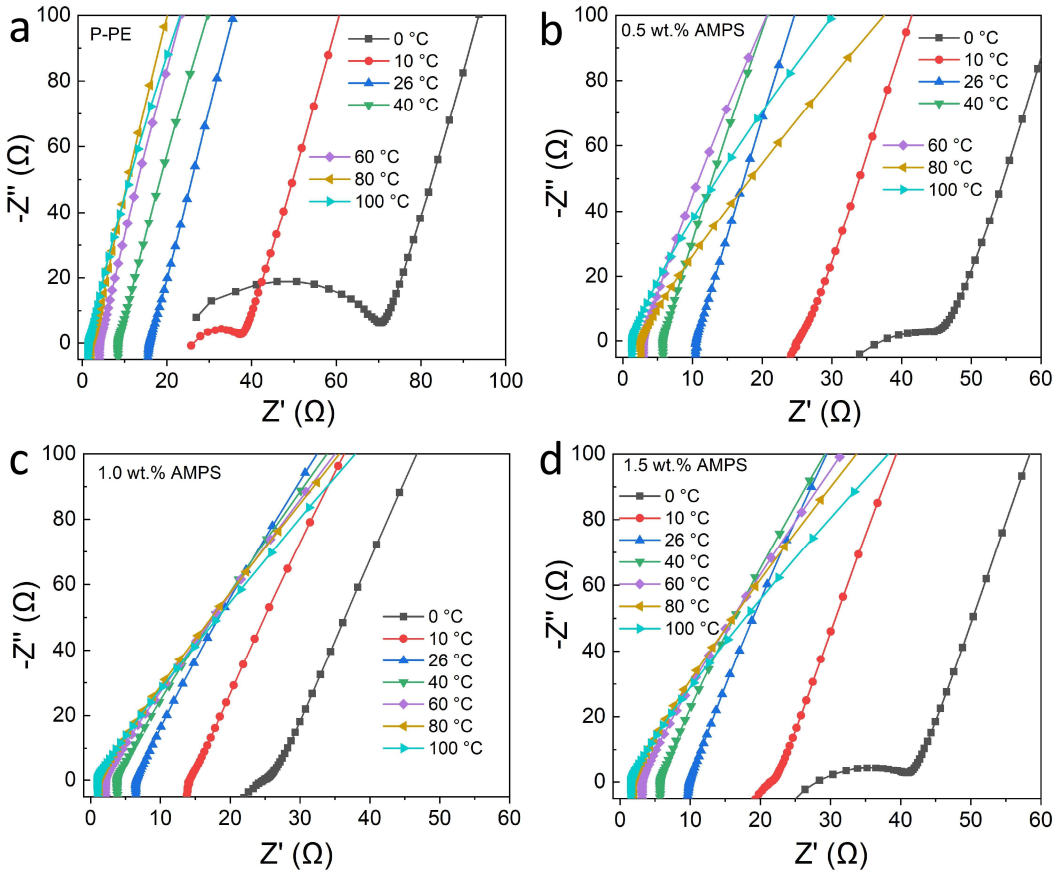

Fig. S2 EIS Nyquist plots of the PVDF-based electrolyte membranes with an AMPS content of (a) 0 wt.%, (b) 0.5 wt.%, (c) 1.0 wt.%, or (d) 1.5 wt.%. The corresponding thicknesses of the electrolytes are 28, 27, 28, and 30 μm, respectively.

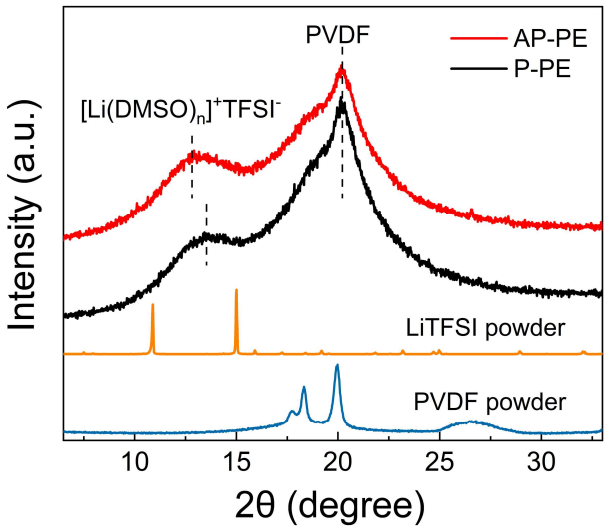

Fig. S3 XRD patterns of PVDF powder, LiTFSI powder, a P-PE, and an AP-PE (1.0 wt.% AMPS). A broad peak at around 13° appears in the XRD patterns of the AP-PE and P-PE can be attributed to the solvated complex $[Li(DMSO)_n]^+TFSI^-$, where *n* is the coordination number between Li^+ and DMSO molecules.[1,2] The peak at 20.1° can be assigned to the crystalline peak of PVDF.[3]

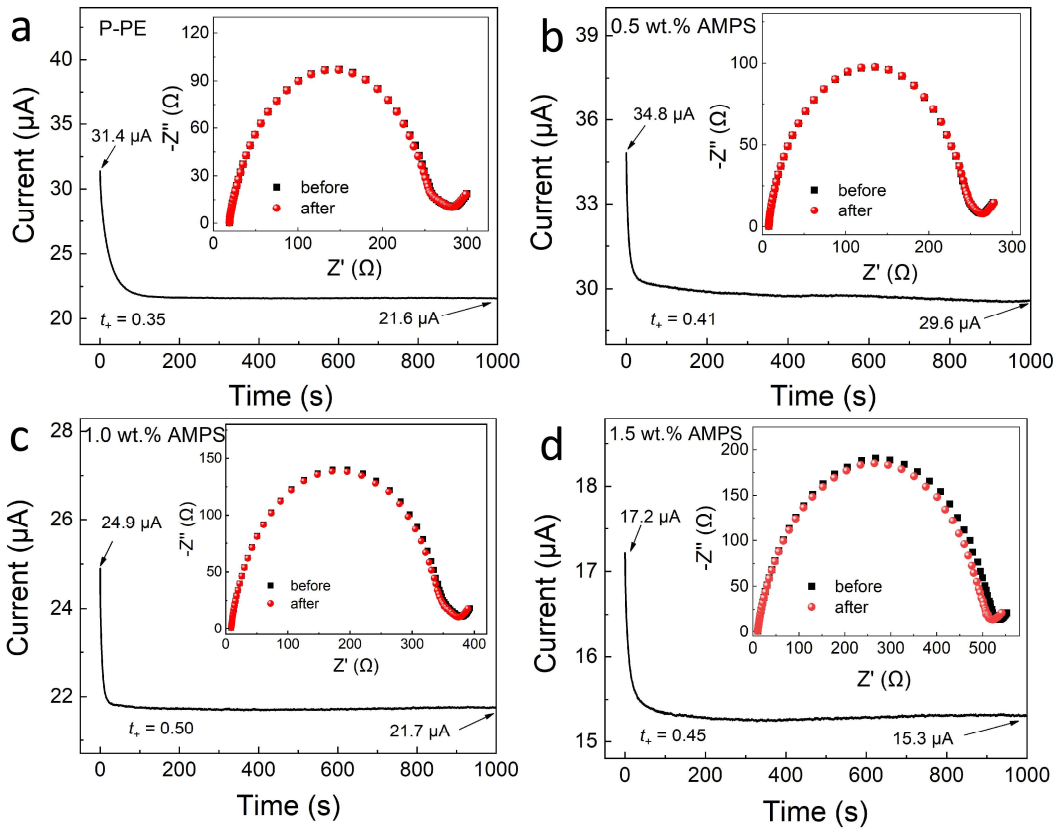

Fig. S4 Current-time profiles of (a) the Li|P-PE|Li symmetric cell and the Li|AP-PE|Li symmetric cells with an AMPS content of (b) 0.5 wt.%, (c) 1.0 wt.%, or (d) 1.5 wt.% with a DC voltage of 10 mV at 26 °C. The insets show the corresponding EIS Nyquist plots before and after polarization. For each case, the data of the sample whose t_+ value is the closest to the mean of the three measurements in Table S3 is used to plot.

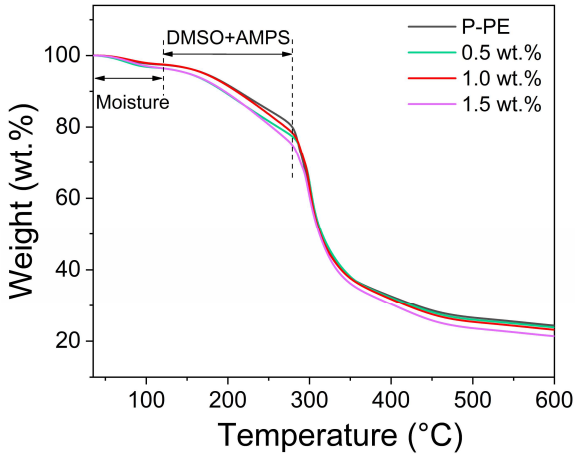

Fig. S5 TGA curves of the P-PE and AP-PE with different contents of AMPS. The contents of DMSO were determined by subtracting the weight of AMPS from the weight loss between the endpoint of the evaporation of moisture and the starting point of the decomposition of LiTFSI.[1,4,5]

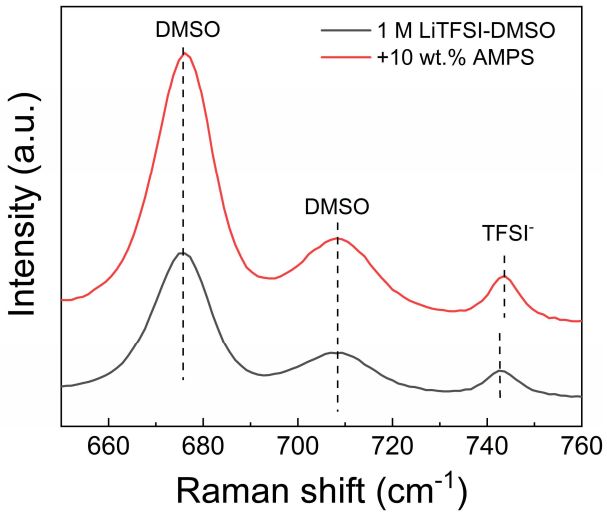

Fig. S6 Raman spectra of the 1.0 M LiTFSI-DMSO mixed solution before (black) and after (red) adding 10.0 wt.% AMPS.

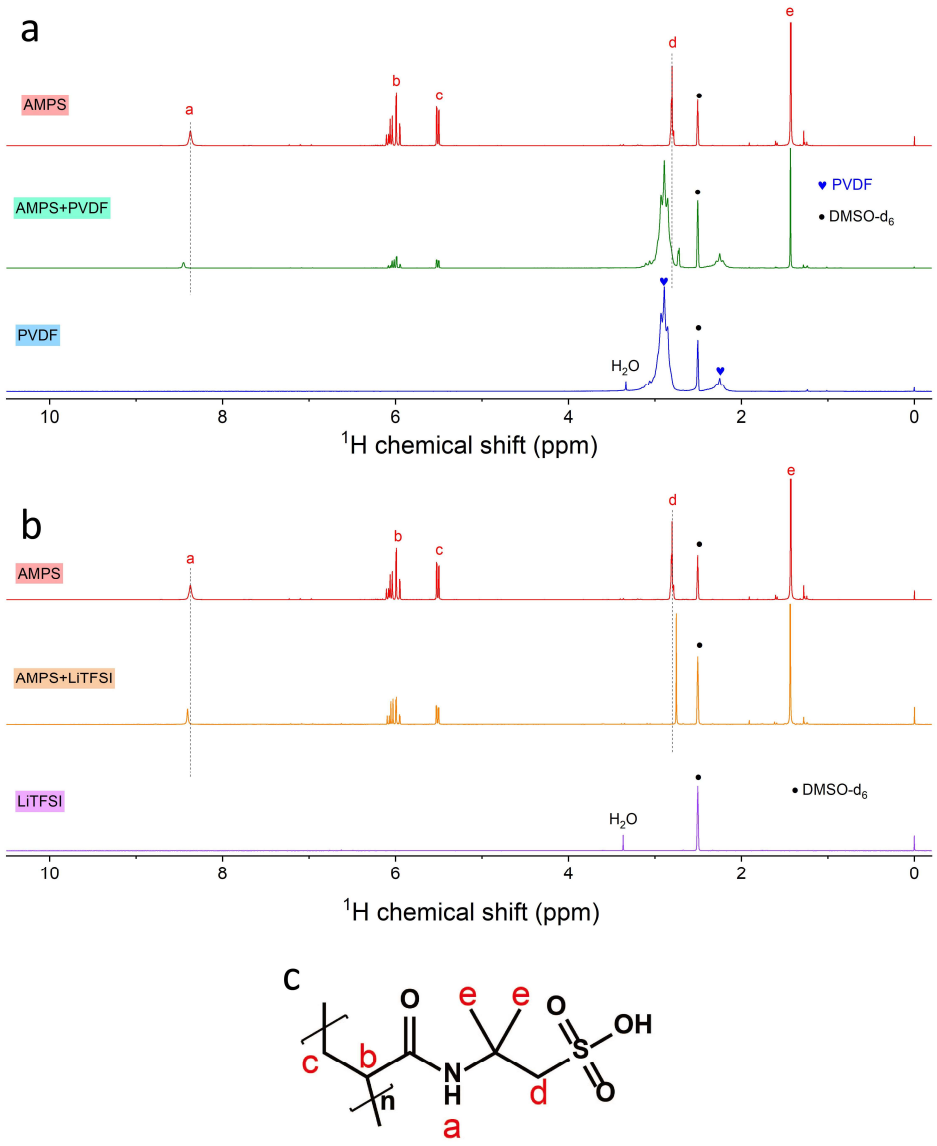

Fig. S7 (a) ^{1}H-NMR full spectra of AMPS, PVDF, and AMPS+PVDF. (b) ^{1}H-NMR full spectra of AMPS, LiTFSI, and AMPS+LiTFSI. DMSO-d_6 was used as the solvent. (c) Structural formula of PAMPS showing the corresponding H atoms that are noted in (a) and (b). When AMPS is added into a PVDF-DMSO-d_6 solution (AMPS+PVDF), the peak *a* for the H atom of –CONH– in AMPS shifts from 8.372 to 8.451 ppm and the peak *d* for the H atoms of –CH_2– in AMPS shifts from 2.802 to 2.725 ppm. When AMPS is added into a LiTFSI-DMSO-d_6 solution (AMPS+LiTFSI), these two peaks (*a* and *d*) shift to 8.404 and 2.753 ppm, respectively.[6] The signal of H_2O comes from the absorbed trace water in PVDF and LiTFSI powder. The samples were prepared by dissolving 5 mg AMPS, 5 mg PVDF, 5 mg LiTFSI, 5 mg AMPS plus 5 mg PVDF, and 5 mg AMPS plus 5 mg LiTFSI powders in 0.6 mL DMSO-d_6, respectively.

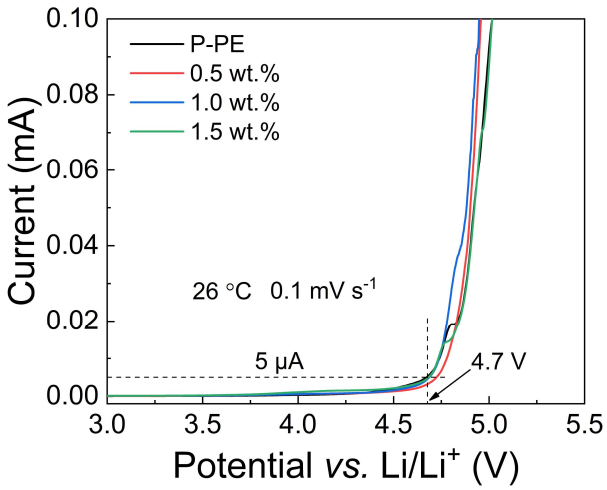

Fig. S8 LSV curves with a scanning speed of 0.1 mV s^{-1} of the electrolyte membranes with different AMPS contents.

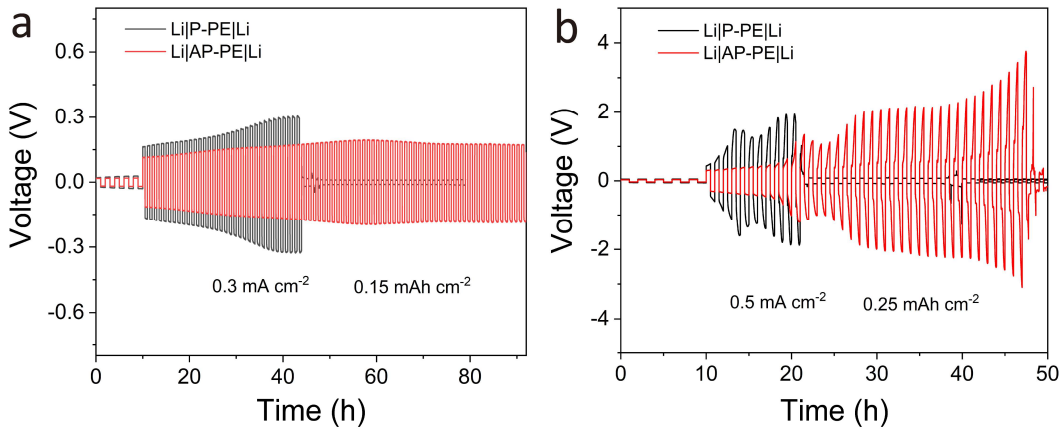

Fig. S9 Cycling tests of the Li|P-PE|Li and Li|AP-PE|Li symmetric cells at (a) 0.3 mA cm^{-2} and 0.15 mAh cm^{-2} and (b) 0.5 mA cm^{-2} and 0.25 mAh cm^{-2}. The cells were cycled at 0.05 mA cm^{-2} and 0.05 mAh cm^{-2} for the first 5 cycles. All the cycling tests were conducted at 26 °C.

Fig. S10 Photographs of the Li electrodes of the Li|AP-PE|Li (left) and Li|P-PE|Li (right) cells after 500 h cycling at 0.1 mA cm^{-2} and 0.1 mAh cm^{-2}.

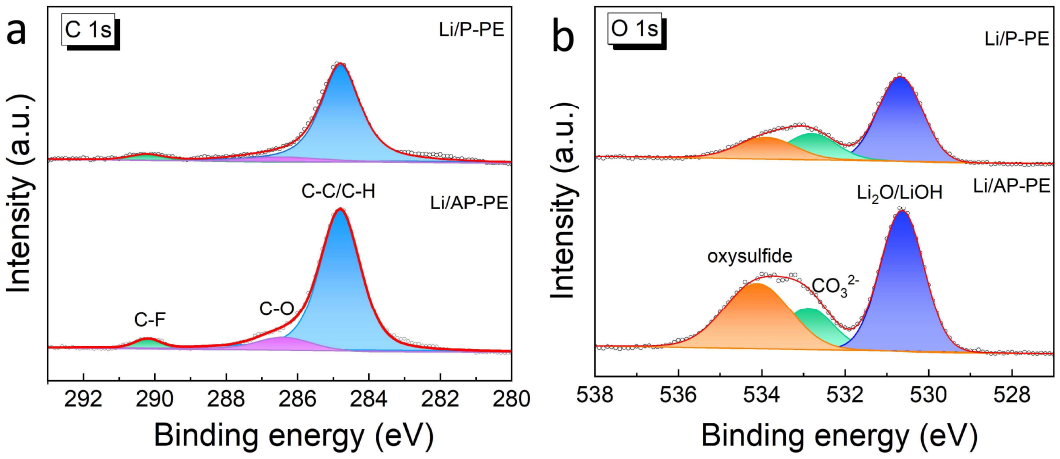

Fig. S11 (a) C 1s and (b) O 1s XPS spectra of the cycled Li foils in the Li|AP-PE|Li and Li|P-PE|Li cells.

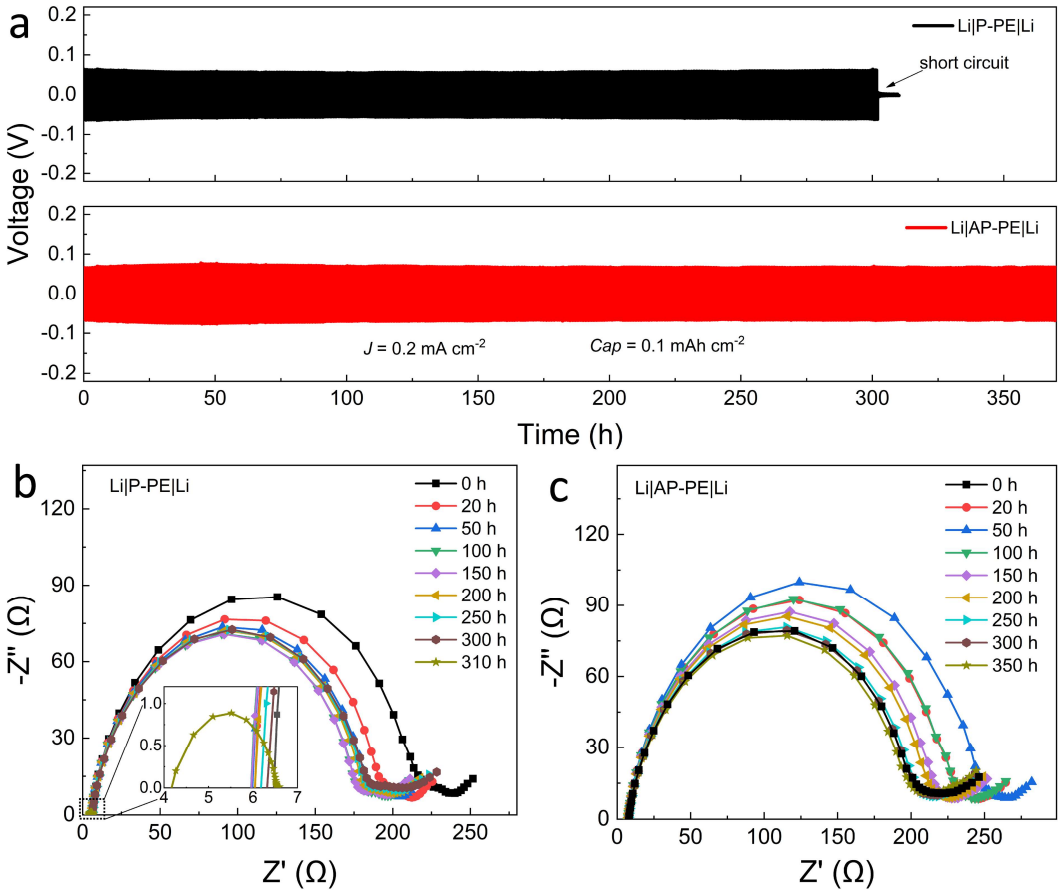

Fig. S12 (a) Galvanostatic Li plating/stripping profiles of the Li|P-PE|Li and Li|AP-PE|Li symmetric cells at 0.2 mA cm^{-2} and 0.1 mAh cm^{-2}. (b, c) Corresponding EIS Nyquist plots of the Li|P-PE|Li and Li|AP-PE|Li symmetric cells at different cycling time, respectively.

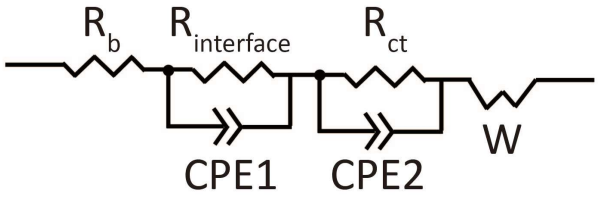

Fig. S13 Equivalent circuit model for the Li|P-PE|Li and Li|AP-PE|Li symmetric cells. There are several components in the EIS Nyquist plots in Figs. S12b and S12c: the intercept on the Z' axis in the high frequency region is assigned to the bulk resistance R_b of the cell; the two quasi-semicircle arcs in the high-to-medium and medium frequency regions are corresponding to the interfacial resistance $R_{interface}$ and charge transfer resistance R_{ct}, respectively; a sloping line at the low frequency region is correlated to the Warburg *W* diffusion resistance. CPE stands for constant phase element.[7]

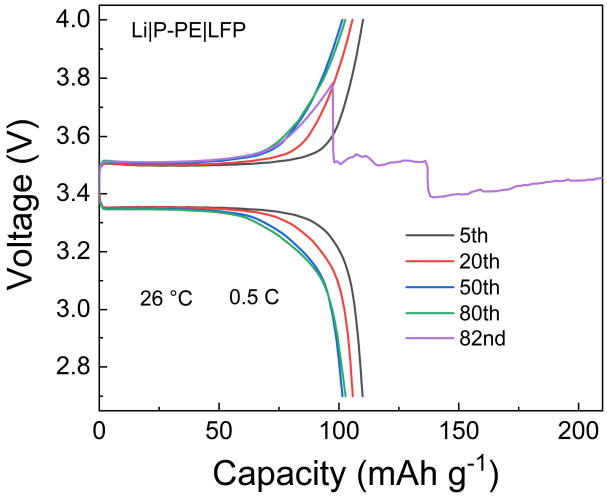

Fig. S14 Charge-discharge voltage profiles of a Li|P-PE|LFP battery with 0.5 C at different cycles. Short circuit occurred at the 82nd cycle.

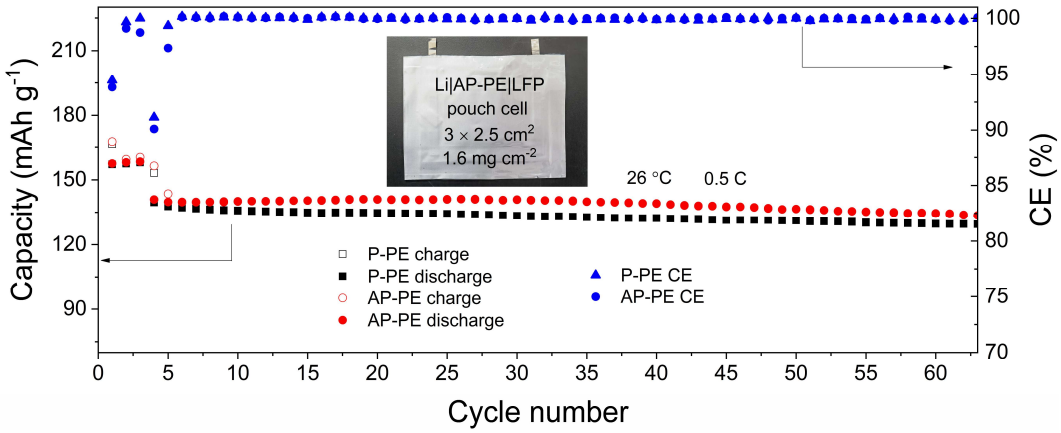

Fig. S15 Cycling performance of the Li|AP-PE|LFP and Li|P-PE|LFP pouch cells at 0.5 C. Before the long-term cycling test, the batteries were initially activated at 0.1 C for 3 cycles. The inset is the photography of the Li|AP-PE|LFP pouch cell.

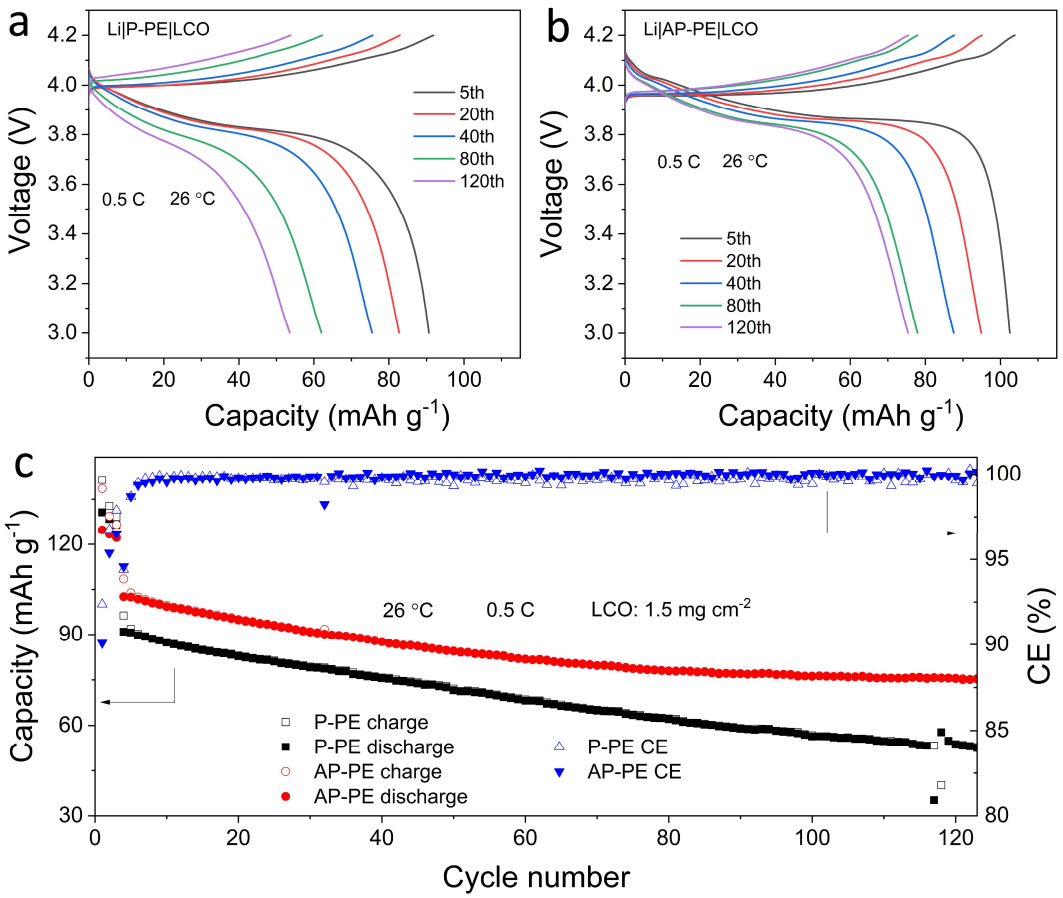

Fig. S16 Charge-discharge voltage profiles of the (a) Li|P-PE|LCO and (b) Li|AP-PE|LCO batteries at 0.5 C (1 C = 140 mA g^{-1}) at different cycles. (c) Long-term cycling performance of the Li|P-PE|LCO and Li|AP-PE|LCO batteries at 0.5 C. Before the long-term cycling test, the batteries were initially activated at 0.1 C for 3 cycles.

Table S1 Molecular weights of PAMPS measured by GPC.

Sample	M_n* (Daltons)	M_w* (Daltons)	M_p* (Daltons)	Polydispersity (M_w/M_n)
AMPS-DMSO solution[a]	4587	9600	9887	2.1
AP-PE with 1.0 wt.% AMPS[b]	6192	8670	9665	1.4
AP-PE with 10.0 wt.% AMPS[b]	7420	9344	10349	1.3

*M_n, M_w, and M_p represent the number-average molecular weight, weight-average molecular weight, and peak-average molecular weight, respectively.

[a]The AMPS-DMSO solution was prepared by adding 30 mg AMPS powder in 8 mL DMSO and stirring the solution at 50 °C for 24 h.

[b]The samples were prepared by re-dissolving the corresponding 40 mg AP-PE membranes in 8 mL DMSO.

Table S2 Comparison of the thickness (*L*), ionic conductivity (σ), and areal conductance (σ/L) of different PVDF-based polymer electrolytes without liquid electrolyte.

Electrolyte	*L* (μm)	σ (mS cm^{-1})	σ/L (mS cm^{-2})	T (°C)	Ref.*
PVDF/$LiClO_4$/DMF	100	0.12	12.0	25	16
PVDF/LiFSI/DMF	90	0.118	13.1	25	17
P(VDF-TrFE-CTFE)/LiTFSI/DMF[a]	70	0.31	44.3	25	19
PVDF/LiTFSI/LLZO/LLTO[b]	60	0.138	23.0	25	25
PVDF/LiTFSI/$3Li_2S{\cdot}2P_2S_5$	40	0.342	85.5	RT	26
PVDF/LiFSI/LATP/DMF[c]	100	0.6	60.0	RT	27
PVDF/LiFSI/PAA/DMF[d]	80	0.091	11.4	30	29
PVDF-HFP/LiTFSI /LLZNO/MOF/PEO[e]	80	0.2	25.0	25	33
PVDF-HFP/LiTFSI/Li_7PS_6	150	0.111	7.4	RT	51
PI/PVDF/LiTFSI/LLZTO[f]	20	0.123	61.5	25	52
PVDF-HFP/LiTFSI/LLATO/Li_3PO_4[g]	80	0.51	63.8	25	53
PVDF/$LiClO_4$/LSTHF/TMP[h]	140	0.53	37.9	23	54
PVDF-HFP/LiTFSI/PEGDME[i]	70	0.34	48.6	RT	55
PVDF/LiTFSI/LiBOB/DMF/EC/PC/FEC[j]	100	0.73	73.0	20	56
PVDF/PEO/LiTFSI/Gd-doped CeO_2	60	0.23	38.3	30	57
PVDF/LiTFSI/porous carbon/NMP	120	0.56	46.7	25	58
PVDF-HFP/LiTFSI/EMIMTFSI/SiO_2[k]	50	0.43	86.0	20	59
PVDF-HFP/SPVDFLiHFP[l]	70	0.284	40.6	RT	60
PVDF/LiTFSI/AMPS/DMSO	**28**	**0.22**	**78.6**	**26**	**This work**

***The reference numbers listed here are corresponding to those in the reference list in the main text.

[a]P(VDF-TrFE-CTFE) represents poly(vinylidene fluoride-*co*-trifluoroethylene-*co*-chlorotrifluoroethylene). [b]LLZO represents $Li_{6.75}La_3Zr_{1.75}Al_{0.25}O_{12}$ and LLTO represents $Li_{0.33}La_{0.56}TiO_{3-x}$. [c]LATP represents $Li_{1.4}Al_{0.4}Ti_{1.6}(PO_4)_3$ nanowires. [d]PAA represents poly(acrylic acid). [e]LLZNO represents $Li_{6.75}La_3Zr_{1.75}Nb_{0.25}O_{12}$, and MOF represents Cu-(1,3,5-benzenetricarboxylic acid)-1 (HKUST-1). [f]PI represents polyimide, and LLZTO represents $Li_{6.75}La_3Zr_{1.75}Ta_{0.25}O_{12}$. [g]LLATO represents $Li_{0.33}La_{0.557}Ti_{0.995}Al_{0.005}O_3$. [h]LSTHF represents $Li_{0.38}Sr_{0.44}Ta_{0.70}Hf_{0.30}O_{2.95}F_{0.05}$, and TMP represents trimethyl phosphate. [i]PEGDME presents polyethylene glycol dimethyl ether. [j]LiBOB represents lithium bis(oxalato)borate, EC represents ethylene carbonate, PC represents propylene carbonate, and FEC represents fluoroethylene carbonate. [k]EMIMTFSI represents 1-ethyl-3-methylimidazolium bis(trifluoromethanesulfonyl)imide. [l]SPVDFLiHFP represents sulfonated polyvinylidene fluoride lithium-hexafluoropropylene.

Table S3 Measured R_0, R_s, I_0, and I_s values in the measurements of Li^+ transference number.

AMPS content (wt.%)	No.	R_0 (Ω)	R_s (Ω)	I_0 (mA)	I_s (mA)	t_+	Average t_+
0	1	190.4	189.5	0.04280	0.02991	0.2986	
0	2	241.8	240.5	0.03138	0.02161	0.3459	0.35
0	3	214.0	204.0	0.03958	0.03321	0.3980	
0.5	1	251.7	251.6	0.03482	0.02958	0.4101	
0.5	2	253.7	252.1	0.03310	0.02805	0.4637	0.42
0.5	3	315.0	312.0	0.02810	0.02403	0.3924	
1.0	1	283.2	282.6	0.02933	0.02439	0.4533	
1.0	2	377.5	373.9	0.02214	0.01928	0.5123	0.49
1.0	3	340.1	336.1	0.02489	0.02175	0.4987	
1.5	1	444.7	443.1	0.01941	0.01621	0.4056	
1.5	2	511.0	496.0	0.01721	0.01532	0.4470	0.44
1.5	3	503.2	494.8	0.01738	0.01538	0.4645	

Table S4 Fitting results of the EIS Nyquist plots of the Li|P-PE|Li and Li|AP-PE|Li symmetric cells in Figs. S12b and S12c based on the equivalent circuit model in Fig. S13.

Li|P-PE|Li				Li|AP-PE|Li			
Time (h)	R_b (Ω)	$R_{interface}$ (Ω)	R_{ct} (Ω)	Time (h)	R_b (Ω)	$R_{interface}$ (Ω)	R_{ct} (Ω)
0	6.224	205.4	25.26	**0**	7.890	193.4	27.20
20	5.839	184.2	20.52	**20**	7.466	221.3	19.84
50	5.808	175.9	21.12	**50**	7.415	238.6	19.51
100	5.823	169.0	21.31	**100**	7.373	220.4	19.83
150	5.841	169.6	20.56	**150**	7.336	209.6	18.26
200	5.883	176.2	19.39	**200**	7.492	202.2	16.14
250	6.070	174.8	24.17	**250**	7.640	195.8	16.81
300	6.195	176.0	38.99	**300**	7.654	194.3	17.36
310	4.468	1.930	0.150	**350**	7.686	191.6	17.91

Table S5 Comparison of the performance of the Li|AP-PE|LFP cell with other reported Li||LFP cells using polymer electrolytes.

Electrolyte	Mass loading (mg cm^{-2})	Initial capacity at 0.5 C (mAh g^{-1})	Capacity after cycling at 0.5 C (mAh g^{-1}@cycles)	T (°C)	Ref.*
P(VDF-TrFE-CTFE)/LiTFSI/DMF[a]	1.6	~ 146.3	144.1@150	25	19
PVDF/LiTFSI/LLZO/LLTO[b]	2.5	150	127@550	RT	25
PVDF-HFP/LiTFSI/LLATO/Li_3PO_4[c]	/	130.7	114.7@160	25	53
PVDF/LiTFSI/LiBOB/DMF/EC/PC/FEC[d]	2–3	151	143@500	23	56
PVDF-HFP/LiTFSI/EMIMTFSI/SiO_2[e]	2.0	135.7	114.9@400	RT	59
PVDF-HFP/LLZO/LiTFSI-TEGDME[f]	2.1–2.3	120	~ 111@180	RT	72
PPC/LiTFSI/CNM[g]	5	~ 116	~ 110@1000	20	73
PEO/LiTFSI/PAN-LLZTO[h]	3.0	~ 70	96.5@400	RT	74
PAN/LiTFSI/EMIMTFSI/SiO_2	2.0	156.5	148.8@500	RT	75
PBPF/PBPO[i]	3.2	~ 139.6	129.8@150	25	76
PVDF/LiTFSI/AMPS/DMSO	**1.8**	**131.2**	**120.3@178**	**26**	**This work**

*****The reference numbers listed here are corresponding to those in the reference list in the main text.

[a]P(VDF-TrFE-CTFE) represents poly(vinylidene fluoride-*co*-trifluoroethylene-*co*-chlorotrifluoroethylene). [b]LLZO represents $Li_{6.75}La_3Zr_{1.75}Al_{0.25}O_{12}$ and LLTO represents $Li_{0.33}La_{0.56}TiO_{3-x}$. [c]LLATO represents $Li_{0.33}La_{0.557}Ti_{0.995}Al_{0.005}O_3$. [d]LiBOB represents lithium bis(oxalato)borate, EC represents ethylene carbonate, PC represents propylene carbonate, and FEC represents fluoroethylene carbonate. [e]EMIMTFSI represents 1-ethyl-3-methylimidazolium bis(trifluoromethanesulfonyl)imide. [f]LLZO represents $Li_7La_3Zr_2O_{12}$ and TEGDME represents tetra ethylene glycol dimethylether. [g]PPC represents poly(propylene carbonate) and CNM represents cellulose nonwoven membrane. [h]PAN-LLZTO represents polyacrylonitrile/$Li_{6.7}La_3Zr_{1.7}Ta_{0.3}O_{12}$ fiber network. [i]PBPF is composed of butyl acrylate (BA), poly-(ethylene glycol) diacrylate (PEGDA), PVDF-HFP, triethyl phosphate and FEC; PBPO is composed of the BA-PEGDA-PEO matrix and EC/DMC (DMC: dimethyl carbonate) plasticizer.

References

1 F. Xu, S. Deng, Q. Guo, D. Zhou and X. Yao, *Small Methods*, 2021, **5**, 2100262.

2 L. Wang, K. Uosaki and H. Noguchi, *J. Phys. Chem. C*, 2020, **124**, 12381–12389.

3 Y. Liang, S. Guan, C. Xin, K. Wen, C. Xue, H. Chen, S. Liu, X. Wu, H. Yuan, L. Li and C. W. Nan, *ACS Appl. Mater. Interfaces*, 2022, **14**, 32075–32083.

4 S. J. Xu, R. G. Xu, T. Yu, K. Chen, C. G. Sun, G. J. Hu, S. Bai, H. M. Cheng, Z. H. Sun and F. Li, *Energy Environ. Sci.*, 2022, **15**, 3379–3387.

5 Y.-F. Huang, T. Gu, G. Rui, P. Shi, W. Fu, L. Chen, X. Liu, J. Zeng, B. Kang, Z. Yan, F. J. Stadler, L. Zhu, F. Kang and Y.-B. He, *Energy Environ. Sci.*, 2021, **14**, 6021–6029.

6 Y. Cai, H. Wu, W. Yan, Z. Yu, W. Ma, C. Liu, Q. Zhang and X. Jia, *ACS Appl. Polym. Mater.*, 2021, **3**, 3254–3263.

7 P. Vadhva, J. Hu, M. J. Johnson, R. Stocker, M. Braglia, D. J. L. Brett and A. J. E. Rettie, *Chemelectrochem*, 2021, **8**, 1930–1947.